THEMED SECTION: MEDIATORS AND RECEPTORS IN THE RESOLUTION OF INFLAMMATION

RESEARCH PAPER

Resolvin D1 controls inflammation initiated by glutathione-lipid conjugates formed during oxidative stress

M Spite[1], L Summers[1], TF Porter[1], S Srivastava[2], A Bhatnagar[2] and CN Serhan[1]

[1]Center for Experimental Therapeutics and Reperfusion Injury, Department of Anesthesiology, Perioperative and Pain Medicine, Brigham and Women's Hospital and Harvard Medical School, Boston, MA, USA, and [2]Institute of Molecular Cardiology, Department of Medicine, University of Louisville, Louisville, KY, USA

Background and purpose: Inflammation is associated with oxidative stress and local generation of lipid peroxidation-derived aldehydes, such as 4-hydroxy-*trans*-2-nonenal (HNE). In most tissues, HNE is readily conjugated with glutathione and presently it is unknown whether glutathionyl-HNE (GS-HNE) plays a functional role in inflammation. Here, we sought to determine whether GS-HNE is a mediator of oxidative stress-initiated inflammation and if its actions can be regulated by the anti-inflammatory and pro-resolving lipid mediator, resolvin D1 (RvD1).

Experimental approach: GS-HNE was administered intraperitoneally to mice and peritoneal lavages were assessed for leukocyte infiltration and lipid mediators were targeted by mediator-lipidomics. RvD1 was administered to mice treated with GS-HNE and leukocyte infiltration was assessed in the peritoneum. Superoxide production and CD11b modulation were measured in isolated human polymorphonuclear leukocytes incubated with GS-HNE.

Key results: GS-HNE (1–10 μg) evoked infiltration of Gr-1$^+$ leukocytes into the peritoneum to form an inflammatory exudate. With isolated human polymorphonuclear leukocytes, GS-HNE stimulated both superoxide generation and CD11b expression. Among the lipid mediators, both cyclooxygenase- and lipoxygenase-derived pro-inflammatory eicosanoids, including prostaglandin E$_2$, leukotriene B$_4$ and cysteinyl leukotrienes, were generated in exudates of mice injected intraperitoneally with GS-HNE. RvD1, given i.v. in doses as low as 0.01–10.0 ng, sharply reduced GS-HNE-stimulated leukocyte infiltration (~30–70%).

Conclusions and implications: Glutathione conjugates of HNE, derived during oxidative stress, are pro-inflammatory *in vivo*. RvD1 protects against this oxidative stress-initiated inflammation.

British Journal of Pharmacology (2009) **158**, 1062–1073; doi:10.1111/j.1476-5381.2009.00234.x; published online 5 May 2009

This article is commented on by Filep, pp. 1059–1061 of this issue and is part of a themed issue on Mediators and Receptors in the Resolution of Inflammation. To view this issue visit http://www3.interscience.wiley.com/journal/121548564/issueyear?year=2009

Introduction

Inflammation is a physiological response to tissue injury and serves as a protective mechanism to clear foreign pathogens from the host (Cotran *et al.*, 1999). The acute inflammatory

response is initiated and then actively resolves to re-establish homeostasis. The development and resolution of inflammation are governed, in part, by temporally and spatially regulated formation and action of enzymatically derived lipid mediators (Serhan *et al.*, 2007a). Cyclooxygenase- and lipoxygenase-mediated conversion of arachidonic acid generates pro-inflammatory lipid mediators [prostaglandins(PGs) and leukotrienes (LTs)], and anti-inflammatory/pro-resolving lipoxins, which have well characterized actions such as the regulation of cellular trafficking, vascular tone and cytokine generation (Yedgar *et al.*, 2007). More recently, lipid mediators biosynthesized from ω-3 fatty acids, such as eicosapentaenoic acid and docosahexaenoic acid (DHA) have been characterized *in vivo* from resolving exudates, termed resolvins (resolution phase interaction products) and protectins (Serhan *et al.*, 2002; Serhan and Chiang, 2008). Resolvins and protectins display potent anti-inflammatory and pro-resolving actions that have been demonstrated in many disease models (Serhan and Chiang, 2008). Interference of these apparently tightly regulated pathways may form the basis for tissue injury and a sustained inflammatory response, characteristic of chronic inflammatory diseases, such as atherosclerosis, Alzheimer's disease and arthritis.

Oxidative stress is a generalized feature of many chronic inflammatory diseases and results in the generation of reactive intermediates that actively promote inflammation (Libby, 2007) or potentially disrupt its natural resolution (Serhan and Chiang, 2008). Among the many targets of oxidative stress-derived reactive oxygen species, polyunsaturated fatty acids are particularly susceptible to free radical attack given the ease of *bis*-allylic hydrogen abstraction. The products of non-enzymatic oxidation of cellular lipids are diverse, resulting in oxygenated rearrangement adducts, such as the isoprostanes, phospholipids with abbreviated side chains and freely diffusible oxygenated fragmentation products, such as the α,β-unsaturated aldehyde, 4-hydroxy-*trans*-2-nonenal (HNE) (Benedetti *et al.*, 1980; Subbanagounder *et al.*, 2000; Milne *et al.*, 2004).

HNE is an abundantly generated unsaturated aldehyde derived from polyunsaturated oxidized lipids and is highly reactive and toxic (Benedetti *et al.*, 1980). HNE can readily form covalent adducts with proteins through Michael addition or Schiff base formation, thereby altering protein function. Most notably, HNE modifies low-density lipoprotein (LDL), rendering the macromolecule immunogenic and pro-inflammatory (Yla-Herttuala *et al.*, 1989). Because of its high reactivity and toxicity, HNE is readily metabolized by most cells via multiple biochemical pathways, including reduction and oxidation. However, the major transformation of HNE in most tissues is by conjugation with reduced glutathione (GSH). In this reaction, GSH spontaneously adds to the electron-deficient C-3 of HNE leading to the formation of stable Michael adducts. This reaction, however, could also be catalysed by glutathione-*S*-transferases (GSTs) and is currently believed to represent a form of detoxification. Conjugation of HNE has been demonstrated *in vivo* and has also been observed in a variety of cell types *in vitro* (Siems *et al.*, 1997; Srivastava *et al.*, 1998; 2000; Siems and Grune, 2003). In addition, the glutathione adduct of HNE (GS-HNE) is generated in humans and in animal models of chronic inflammatory dis-

eases and is used as a marker of oxidative stress (Volkel *et al.*, 2005; 2006). Moreover, we have previously shown that intracellular GS-HNE stimulates smooth muscle cell growth *in vitro* (Ramana *et al.*, 2006). Although by removing the α,β double bond, conjugation attenuates the chemical reactivity of HNE, it is not clear whether it affects the biological activity of this aldehyde as well. While conjugation increases the water solubility of HNE and primes it for active extrusion via specific membrane transporters (e.g. by multi-drug resistance protein), it also provides structural features that could be recognized by specific receptors for sensing oxidative stress or inflammation. Here, we report that GS-HNE is a potent pro-inflammatory stimulus *in vivo* and that it also has direct action on isolated human polymorphonuclear leukocytes (PMN). These pro-inflammatory actions of GS-HNE were sharply diminished by resolvin D1 (RvD1) *in vivo*.

Methods

Production and qualification of HNE, GS-HNE and GS-DHN

HNE was synthesized and was used to prepare GS-HNE and GS-DHN as reported before (Srivastava *et al.*, 1998). Briefly, the GS-HNE was prepared by incubating 1 μmol of HNE with 5 μmol of GSH in 0.1 mol·L^{-1} potassium phosphate, pH 7.0, for 30 min at room temperature. The reaction was monitored by following the consumption of HNE at 224 nm. The GS-HNE conjugate was isolated by reverse phase (RP)-HPLC using a Varian RP ODS C18 column pre-equilibrated with 0.1% aqueous trifluoroacetic acid. The compounds were eluted using a gradient consisting of solvent A (0.1% aqueous trifluoroacetic acid) and solvent B (100% acetonitrile) at a flow rate of 1 mL·min^{-1}. The gradient was established such that solvent B reached 24% in 20 min, 26% in 30 min and was held at this value for 10 min. In the next 10 min, solvent B reached 60%, and in an additional 5 min it reached 100% and was held at this value for 10 min. The chemical identity of GS-HNE was established by electrospray ionization mass spectrometry (ESI/MS) using a MicroMass ZMD 2000 mass spectrometer (Waters-Micromass, Milford, MA) as described before (Ramana *et al.*, 2006). The concentration of GS-HNE was determined using GS-HNE synthesized from [³H]-HNE for HPLC analysis, as well as d$_{11}$-HNE as an internal standard for ESI/MS. For the synthesis of the reduced form of the glutathione-HNE conjugate (GS-DHN), 100 nmol of GS-HNE was incubated with 300 nmol of NADPH and 100 μg of human recombinant aldose reductase in 0.1 mol·L^{-1} potassium phosphate, pH 6.0, for 3 h at 37°C. The reaction was monitored by following the consumption of NADPH at 340 nm. At the end of the incubation, the GS-DHN conjugate was isolated by RP-HPLC, characterized by ESI$^+$/MS and quantified as described above.

Murine peritonitis

All animal care and experimental procedures were in accordance with the Harvard Medical Area Standing Committee on Animals protocol 02570. Peritonitis was assessed as described by Winyard and Willoughby (2003). Male FVB mice (6–8 weeks old; Charles River, Wilmington, MA) were injected

intraperitoneally (i.p.) with sterile saline (1 mL), GS-HNE (1–10 μg in 1 mL sterile saline), GS-DHN (10 μg) or HNE (10 μg) after anaesthesia with isoflurane. LTB$_4$ and *n*-formylmethionylleucylphenylalanine (fMLP) were also injected i.p. in sterile saline (0.1% EtOH) in parallel analyses with GS-HNE (each administered at 1 μg). In some experiments, RvD1 (0.01–10.0 ng in 100 μL sterile saline) or vehicle control (1.0% EtOH in sterile saline) were injected via the tail vein immediately before GS-HNE (10 μg, i.p.). For determination of the recovery of GS-HNE from the peritoneum, 68 nmol of [^{3}H]GS-HNE (specific activity 3870 cpm·nmol^{-1}) was injected i.p. in 1 mL sterile saline and the lavage (5 mL) was collected at 0, 10, 30 and 240 min post injection. The radioactivity was determined in 500 μL aliquots of the lavage using a scintillation counter and the remaining sample was analysed by RP-HPLC, followed by scintillation counting. In some experiments, the material eluting from the HPLC was subjected to ESI/MS analysis as described above. For assessing leukocyte infiltration, peritoneal lavage was carried out after 4 h (or at indicated time points), cell viability was determined by Trypan blue exclusion and lavaged cells were enumerated by light microscopy. For differential leukocyte counts, lavages were each combined with 15% BSA and centrifuged onto microscope slides at 140× *g* for 4 min using a Cytofuge (StatSpin, Norwood, MA). After drying, the slides were stained with Wright–Giemsa (Sigma) and differential leukocyte counts were determined by morphology via light microscopy. In parallel, the lavages were centrifuged at 480× *g* for 10 min at 25°C and cell pellets were resuspended in DPBS without Ca^{2+} and Mg^{2+} (5% FBS) and incubated with PE-conjugated anti-Gr-1 or IgG isotype control at 4°C for 20 min in the dark. After incubation, the cells were washed and fixed with 3% formalin, followed by FACS analysis using a FACsort (Becton-Dickinson Co.) and Cellquest software. In some experiments, the peritoneal lining was obtained for histological evaluation. For this purpose, punch biopsies were placed in 3% neutral formalin and sections were processed and stained (haematoxylin and eosin) by the Department of Pathology core at Children's Hospital Boston.

Assessment of vascular permeability
Mice were injected with Evan's blue dye (1% in 100 μL DPBS, i.v.) immediately before i.p. injection of GS-HNE (10 μg) or LTD$_4$ (100 ng). After 15 min, mice were anaesthetized and peritoneal lavages were obtained. After centrifugation at 400× *g* for 10 min, the OD$_{610}$, with a background reference at 450 nm, of the supernatants was determined using a spectrophotometer.

Isolation of human PMNs and superoxide generation
Human PMNs were isolated from healthy donors who abstained from taking any medication for 2 weeks prior to donation, by Ficoll gradient, using the Brigham and Women's Hospital protocol # 88-02642. Superoxide anion generation was determined as described by Hasturk *et al.* (2006). Briefly, freshly isolated PMNs (1.5 × 10^6 cells per incubation) in DPBS (with 0.9 mmol·L^{-1} CaCl$_2$ and 0.5 mmol·L^{-1} MgCl$_2$) were incubated alone or with GS-HNE (1–10 μmol·L^{-1}) at 37°C for

10 min. The reduction of ferricytochrome *c* was determined spectrophotometrically (OD$_{550}$). In some experiments, superoxide dismutase (SOD; 30 μg·mL^{-1}) was added immediately before GS-HNE. fMLP (50 nmol·L^{-1}) was used as a positive control.

Regulation of CD11b
Freshly isolated human PMNs (2 × 10^6 cells per incubation) were incubated alone or with GS-HNE (10 μmol·L^{-1}) in DPBS at room temperature for 15 min. Upon incubation, the cells were centrifuged at 480× *g* for 10 min at 4°C without a brake to prevent cell activation. After fixing (3% formalin) and washing in DPBS, the cells were stained with either IgG isotype control or FITC-conjugated anti-CD11b for 1 h at 4°C in the dark. After washing, the cells were taken for FACS analysis (Fiore and Serhan, 1995).

Mediator lipidomics
Mice were injected with sterile saline (1 mL) or GS-HNE (10 μg in 1 mL) and the peritoneum was lavaged (5 mL) after 4 h with DPBS. Immediately following, 2 volumes of cold methanol, containing 400 pg of d4-PGE$_2$ as an internal standard, was added to exudates and the samples were cooled to –20°C for 30 min to allow protein precipitation. The samples were then centrifuged at 850× *g* for 20 min (4°C) and supernatants were taken for solid-phase extraction using C18 SEP-PAK cartridges (Alltech, Deerfield, IL). Methyl formate fractions were taken to dryness with a gentle stream of N$_2$ and the samples were resuspended in methanol for LC/MS/MS analysis as described by Hong *et al.* (2008). Briefly, isolated material was injected into an HPLC-UV (Agilent 1100) coupled to an ion-trap mass spectrometer (QTrap 3200; Applied Biosystems/Sciex) equipped with a C18 column (Agilent Eclipse Plus, 4.6 mm × 50 mm × 1.8 μm). The mobile phase consisted of methanol/water/acetic acid (60/40/0.01; v/v/v) and was ramped to 80/20/0.01 (v/v/v) over 5 min, to 95/5/0.01 (v/v/v) over the next 3 min and to 100/0/0.01 (v/v/v) over 6 min before returning to 60/40/0.01 (v/v/v) at a flow rate of 0.4 mL·min^{-1}. Lipid mediators of interest were profiled using multiple reaction monitoring and identified by direct comparison with synthetic standards using retention time and six diagnostic ions and matching criteria (Serhan *et al.*, 2007b). Relative amounts of lipid mediators were calculated based on external calibration curves for each mediator of interest after determination of extraction recovery using the deuterium-labelled internal standard (d4-PGE$_2$) and are expressed as ng lipid mediator per exudate.

Analysis of cysteinyl leukotriene generation *in vivo*
To monitor the production of cysteinyl leukotrienes (cysLT) in response to GS-HNE stimulation, GS-HNE (10 μg) was injected into mice (i.p.) and exudates were collected at indicated time intervals and extracted as described above. After solid-phase extraction, methanol fractions were dried under N$_2$ and the samples were resuspended in extraction buffer for analysis of cysLTs by ELISA according to the manufacturer's instructions.

Statistical analysis
Results are presented as mean ± SEM. Multiple comparisons were analysed by one-way ANOVA, followed by Bonferroni

post-test with $P < 0.05$ considered to be significant. An unpaired Student's *t*-test was used to determine statistical significance of GS-HNE versus GS-HNE plus SOD, as indicated.

Materials

Resolvin D1 (7*S*, 8*R*, 17*S*-trihydroxy-4*Z*,9*E*,11*E*,13*Z*,15*E*,19*Z*-DHA) was prepared by total organic synthesis (Sun *et al.*, 2007). LTB$_4$, LTD$_4$, deuterium labelled (d$_4$) PGE$_2$ and all LC/MS/MS standards were purchased from Cayman Chemical (Ann Arbor, MI). Each lipid mediator was subject to characterization by LC/MS/MS for structural integrity and to establish concentration as described by Serhan *et al.* (2007b). ELISA kits for cysLTs were purchased from Neogen (Lexington, KY). FITC-conjugated anti-human CD11b antibodies were purchased from eBioscience (San Diego, CA) and PE-conjugated anti-mouse Gr-1 antibodies (RB6-8C5) and their IgG isotype controls were purchased from BD Biosciences (Pharmingen; San Jose, CA).

Results

Production and qualification of GS-HNE and GS-DHN

During metabolism, HNE is rapidly conjugated to GSH in a reaction that is greatly accelerated by GSTs. This reaction yields GS-HNE (Figure 1A), which can either be actively extruded from the cell or reduced by aldose reductase to generate the reduced conjugate, namely GS-DHN. In the studies reported here, the products of the spontaneous reaction were used to represent the products generated *in vivo,* as multiple GSTs participate in HNE metabolism and spontaneous glutathiolation can also occur. Thus, to evaluate the bioactivity of non-conjugated HNE relative to its GSH conjugates, we synthesized racemic GS-HNE at positions 3 and 4 (see *Methods*). A representative radioplot (Figure 1B) demonstrates the conversion of non-conjugated [³H]HNE to [³H]GS-HNE, which was used to quantify the unlabelled GS-HNE. Fractions corresponding to GS-HNE eluting from the HPLC were further analysed by ESI⁺/MS. As shown in
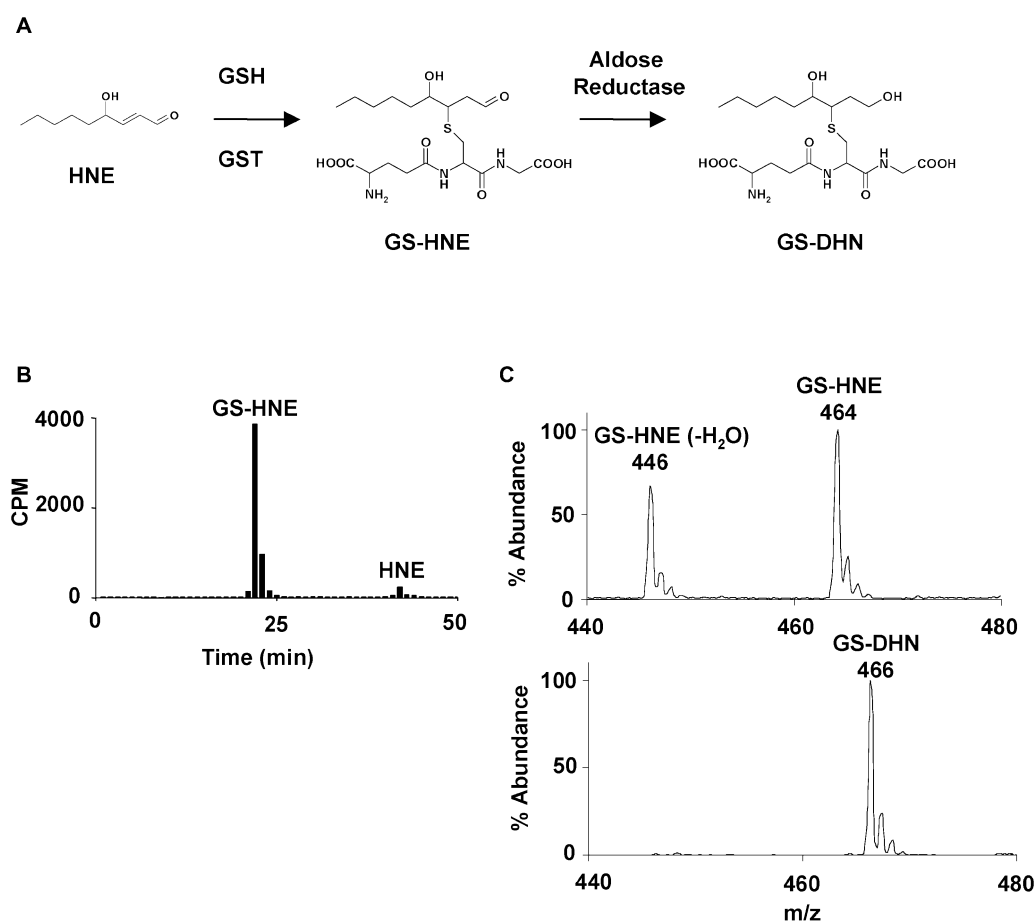

Figure 1 Production and quantification of GS-HNE and GS-DHN. HNE is conjugated to glutathione (GSH) via catalysis by glutathione-*S*-transferases (GSTs) to generate GS-HNE. GS-HNE can then be actively extruded from the cell, or further metabolized to GS-DHN by aldose reductase prior to extrusion (A). GS-HNE was prepared from reacting HNE with GSH and the product was isolated by HPLC and quantified based on [³H]GS-HNE, as shown in the representative radioplot (B). The HPLC-purified product was analysed by ESI⁺/MS (C; upper panel) and displayed an ion at m/z 464 [M+H]⁺ corresponding to GS-HNE, as well as an ion at m/z 446 [M+H]-H$_2$O. Isolated GS-HNE was reduced using human recombinant aldose reductase and the isolated product gave a mass spectrum consistent with reduction of GS-HNE to GS-DHN (m/z 466), as shown by a 2 D increase (C; lower panel). GS-DHN, glutathionyl-1,4-dihydroxynonanol; GS-HNE, glutathionyl-4-hydroxy-*trans*-2-nonenal.

Figure 1C (upper panel), reagent GS-HNE shows an ion at m/z 464 [M+H]$^+$, corresponding to GS-HNE, as well as an ion at m/z 446 ([M+H]-H$_2$O) resulting from the loss of one molecule of water. After reduction of reagent GS-HNE with human recombinant aldose reductase, analysis of the mass spectrum obtained for the isolated material showed a prominent and exclusive ion at m/z 466 [M+H]$^+$ (Figure 1C lower panel). This increase of 2 D was consistent with reduction of the aldehyde to an alcohol.

GS-HNE stimulates acute peritonitis

To determine the potential pro-inflammatory agonist properties of HNE and its GSH conjugates, namely GS-HNE and GS-DHN, the compounds were each administered to mice at a dose of 10 μg by i.p. injection. After 4 h, the peritoneal lavage was collected and the number of infiltrating leukocytes was determined. As shown in Figure 2A, injection of GS-HNE significantly increased peritoneal PMNs, compared with the saline control ($P < 0.001$). The magnitude of this response was nearly 10-fold greater than that to free HNE or the reduced GSH conjugate, GS-DHN ($P < 0.001$ GS-HNE vs. GS-DHN and GS-HNE vs. HNE by one-way ANOVA; Figure 2A). In addition to microscopic evaluation of PMNs, lavage cells were also analysed by FACS using PE-conjugated anti-Gr-1 antibodies. As shown in Figure 2B, injection of GS-HNE resulted in the infiltration of Gr-1$^+$ leukocytes, while virtually no positive staining was observed after saline treatment.

Characterization of GS-HNE-stimulated murine peritonitis

To better assess the potential of GS-HNE as a pro-inflammatory stimulus, we next evaluated the kinetics of the peritoneal leukocyte infiltration stimulated by GS-HNE. As shown in Figure 3, injection of GS-HNE (10 μg i.p.) resulted in a biphasic increase of PMNs in exudates that was significant at both 4 and 24 h ($P < 0.01$ vs. saline by one-way ANOVA) with successive falls in peritoneal PMN numbers at 6 and 12 h. After reaching a minimum at 12 h, a second increase in PMN infiltration was observed reaching a global maximum at 24 h. Similar results were obtained by FACS analysis (Figure 3B) in which a biphasic infiltration of Gr-1$^+$ cells is evident and reflective of the total PMN counts during the time course. We next examined the recovery of GS-HNE during peritonitis, as described in *Methods*. As shown in Figure 3C, [^{3}H]GS-HNE was rapidly cleared from the peritoneal cavity, with about 50% remaining after 10 min, 20% remaining after 30 min, and virtually none remaining after 240 min. Analysis of the lavage by RP-HPLC demonstrated that only fractions corresponding to the GSH conjugates of HNE (see Figure 1 for reference) contained radioactivity (data not shown). As this does not rule out conversion of GS-HNE to GS-DHN, we next analysed the HPLC-isolate by ESI/MS. Mass spectral analysis at 30 min post injection revealed that GS-HNE remained untransformed (m/z 464) and was not reduced to GS-DHN (m/z 466), as was to be expected for this non-cell permeable conjugate (Figure 3D).

Last, in order to evaluate the potency of GS-HNE as a pro-inflammatory stimulus, two different doses were tested in parallel. As shown in Figure 3E, an increase in peritoneal PMN

infiltration was observed with administration of both 1 and 10 μg GS-HNE, although only the 10 μg dose reached statistical significance ($P < 0.05$) over saline injection alone. A representative histological Wright–Giemsa stain of the lavaged cells is shown in Figure 3F.
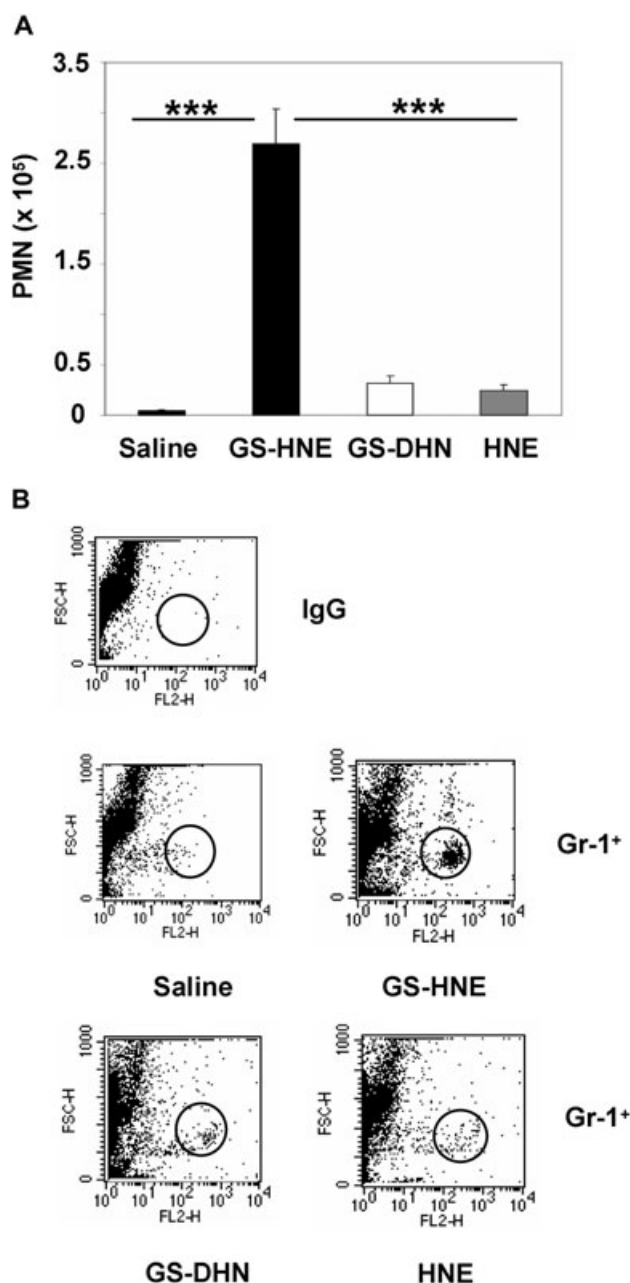

Figure 2 GS-HNE stimulates acute peritonitis. To assess murine peritonitis, GS-HNE, free HNE or GS-DHN were injected intraperitoneally (each 10 μg) and the lavage was collected after 4 h. Total PMNs were determined by differential analysis using Wright–Giemsa staining (A) and confirmed by FACS analysis using PE-conjugated anti-Gr-1 antibodies (B; GS-HNE>>>GS-DHN>HNE). Results are presented as mean ± SEM and are representative of at least three independent experiments (n = 3–4) ***P < 0.001. GS-DHN, glutathionyl-1, 4-dihydroxynonanol; GS-HNE, glutathionyl-4-hydroxy-*trans*-2-nonenal; PMN, polymorphonuclear leukocyte.
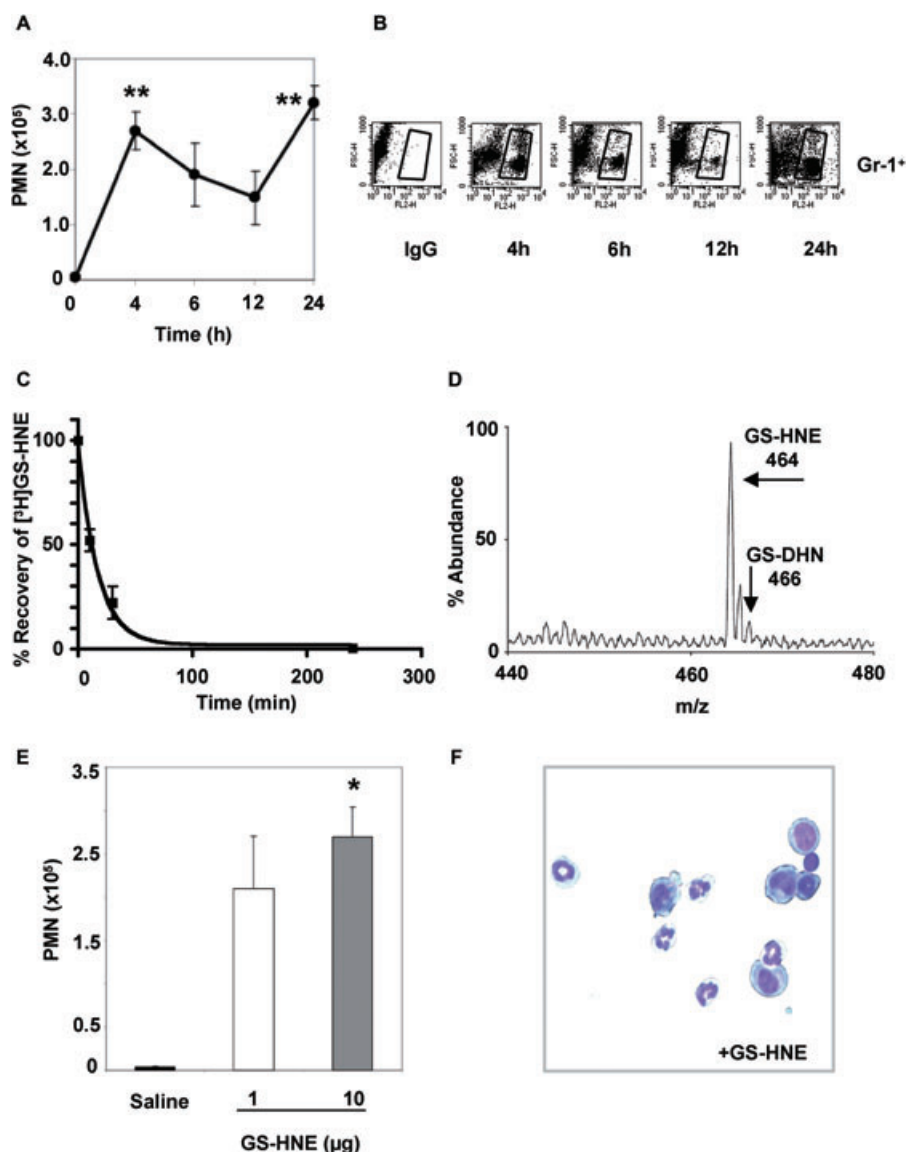
Figure 3 Characterization of GS-HNE-stimulated murine peritonitis. GS-HNE (10 μg) was injected intraperitoneally and peritoneal lavages were collected at indicated times. Total PMNs (A) were determined by differential analysis using Wright–Giemsa staining. In parallel, cells were stained with PE-conjugated anti-Gr-1 antibodies or IgG isotype control and used for FACS analysis (B). The recovery of [^{3}H]GS-HNE from the peritoneal cavity was determined in the lavage at 0, 10, 30 and 240 min post injection (C). A representative mass spectrum of GS-HNE recovered from the peritoneum at 30 min post injection is shown in (D). For determining potency, GS-HNE was injected intraperitoneally at dose of 1 or 10 μg per mouse and exudates obtained after 4 h. Total leukocytes were determined by light microscopy and total PMNs (E) were determined as described above (representative histology shown in F). Results are presented as mean ± SEM ($n = 3$–5), *$P < 0.05$, **$P < 0.01$ (vs. saline by one-way ANOVA). GS-DHN, glutathionyl-1,4-dihydroxynonanol; GS-HNE, glutathionyl-4-hydroxy-*trans*-2-nonenal; PMN, polymorphonuclear leukocyte.

Murine peritonitis: direct comparison of GS-HNE with LTs and fMLP

As the results shown in Figures 2 and 3 demonstrated that GS-HNE was a stimulus for peritoneal leukocyte infiltration, GS-HNE was directly compared with the well-characterized neutrophil chemoattractants and agonists, LTB$_4$ and fMLP. In a parallel comparison (each at 1 μg i.p.), GS-HNE (2.2 nmol; Figure 4A) stimulated peritoneal PMN infiltration ($P < 0.05$ vs. saline) to an extent that was within the range of that stimulated by LTB$_4$ (3 nmol; $P < 0.01$ vs. saline; Figure 4A). Administration of the synthetic peptide, fMLP (2.3 nmol) resulted in PMN infiltration ($P < 0.001$ vs. saline) which, although higher

in magnitude than either GS-HNE or LTB$_4$, was still within the range of these stimuli in this direct comparison.

As increased vascular permeability precedes PMN extravasation, we next determined if GS-HNE was a direct vasoactive agent with a side-by-side comparison with LTD$_4$. In a dose that was 100 times higher than LTD$_4$, GS-HNE (10 μg) did not cause a statistically significant increase in vascular permeability compared with saline at 15 min post injection (Figure 4B), as assessed by Evan's blue dye extravasation (see *Methods*). Only a small increase in permeability was apparent, although this could be a result of local generation of secondary mediators (*vide infra*). By direct comparison, LTD$_4$ stimulated a
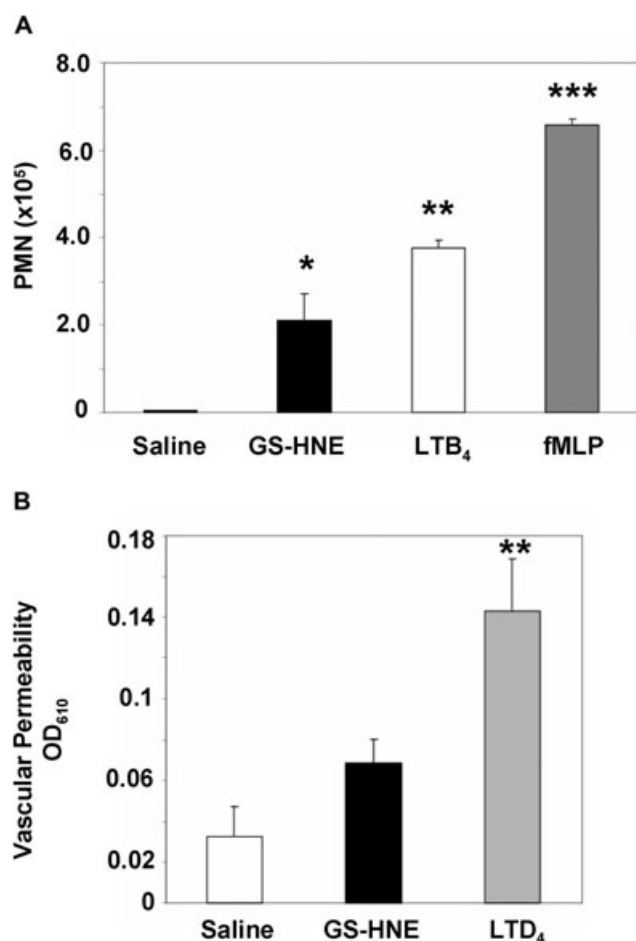
A

B

Figure 4 Murine peritonitis: direct comparison of GS-HNE with LTs and fMLP. GS-HNE, LTB₄ or fMLP were injected intraperitoneally (1 μg each) and lavages were collected after 4 h. Total PMNs were determined by differential analysis using Wright–Giemsa stain and light microscopy (A). For assessment of vascular permeability (B), Evan's blue dye (1%) was injected i.v., followed by intraperitoneal injection of GS-HNE (10 μg; black bar) or LTD₄ (100 ng; grey bar) and the absorbance (OD₆₁₀) of the peritoneal lavage was determined after 15 min. Results are presented as mean ± SEM ($n = 3$–5), *$P < 0.05$, **$P < 0.01$, ***$P < 0.001$ (all vs. saline). fMLP, *n*-formylmethionylleucylphenylalanine; GS-DHN, glutathionyl-1,4-dihydroxynonanol; GS-HNE, glutathionyl-4-hydroxy-*trans*-2-nonenal; LT, leukotriene; PMN, polymorphonuclear leukocyte.

leakage permeability that reached statistical significance at a dose of just 100 ng (Figure 4B; $P < 0.01$ vs. saline).

GS-HNE is a direct PMN agonist

Having demonstrated that GS-HNE is a potent acute pro-inflammatory stimulus *in vivo*, we next sought to determine if GS-HNE has direct action on PMNs. For these experiments, human PMNs were isolated from healthy donors as described in the *Methods*. Isolated PMNs were incubated with GS-HNE (at indicated concentrations) and superoxide anion generation was determined. As shown in Figure 5A, GS-HNE stimulated a statistically significant increase in superoxide generation by human PMNs at all doses tested. Using the maximal concentration from these experiments (10 μmol·L⁻¹), we also determined that this increase in superoxide was inhib-
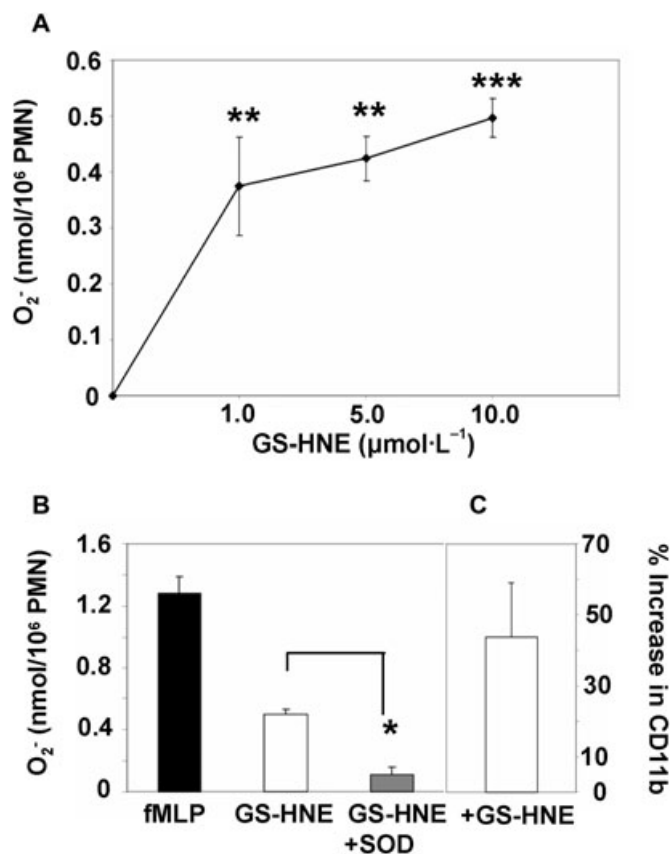
A

B   **C**

Figure 5 GS-HNE stimulation of human PMNs: generation of superoxide anion and modulation of CD11b. Human PMNs were isolated from healthy volunteers as described in *Methods* and incubated with indicated concentrations of GS-HNE (A) for 10 min at 37°C. The superoxide dismutase (SOD)-inhibited reduction of ferricytochrome *c* was monitored spectrophotometrically at 550 nm. The increase in superoxide generation stimulated by GS-HNE (10 μmol·L⁻¹) was inhibited by SOD (B). fMLP (50 nmol·L⁻¹) was used as a positive control. (C) represents the modulation of CD11b expression upon treatment with GS-HNE (10 μmol·L⁻¹; 15 min) as determined by FACS. Results are presented as mean ± SEM (cells from three separate donors), *$P < 0.05$ (vs. GS-HNE by unpaired Student's *t*-test) and **$P < 0.01$ (vs. saline), ***$P < 0.001$ (vs. saline) by one-way ANOVA. GS-DHN, glutathionyl-1,4-dihydroxynonanol; GS-HNE, glutathionyl-4-hydroxy-*trans*-2-nonenal; PMN, polymorphonuclear leukocyte.

ited on prior addition of SOD to the incubations (Figure 5B; $P < 0.05$ to GS-HNE alone), suggesting that GS-HNE directly stimulates increases in superoxide anion generation. Importantly, fMLP (50 nmol·L⁻¹) was used as a positive control in these experiments as an indicator of cell responsiveness for each donor (Figure 5B). As another marker of direct actions on human PMNs, adhesion receptor modulation was assessed. Exposure of human PMNs to GS-HNE (10 μmol·L⁻¹) gave an increase in the surface expression of CD11b compared with vehicle control (DPBS) as determined by FACS (43.7 ± 15.3 %; data from three separate donors; Figure 5C).

GS-HNE stimulates local production of pro-inflammatory lipid mediators in vivo

To determine if stimulation with GS-HNE *in vivo* leads to the secondary generation of pro-inflammatory mediators, we first
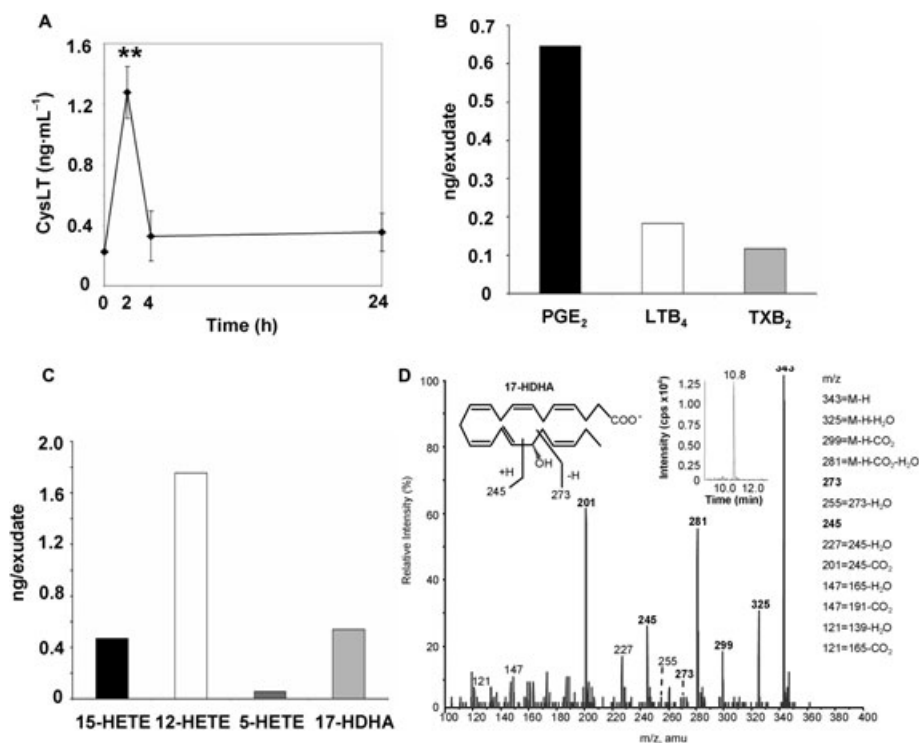
Figure 6 GS-HNE stimulates local production of pro-inflammatory lipid mediators *in vivo*. Mice were injected intraperitoneally with GS-HNE (10 µg) and peritoneal exudates were obtained after 4 h or at indicated time points and the production of lipid mediators was determined (see *Methods*). Cysteinyl leukotrienes were determined by ELISA (A). Mediator lipidomics was carried out by LC/MS/MS to identify pro-inflammatory lipid mediators LTB_4, PGE_2 and thromboxane B_2 (TXB_2) (B). Monohydroxy fatty acids including 5-, 12- and 15-HETE, as well as 17-HDHA were also identified (C). A representative mass spectrum showing the identification of resolvin pathway marker, 17-HDHA, is presented in (D) and the structural diagnostic ions and the chromatogram (MRM) shown in the inset. Results are presented as mean ± SEM, **$P < 0.01$ (vs. 0, 4 and 24 h by one-way ANOVA). GS-HNE, glutathionyl-4-hydroxy-*trans*-2-nonenal; HETE, hydroxyeicosatetraenoic acid; 17-DHA, 17-hydroxy-DHA.

determined if cysLTs were generated. For these experiments, peritoneal lavages from GS-HNE-stimulated mice were collected at indicated time points, extracted and the presence of cysLTs was determined. As shown in Figure 6A, an increase in cysLTs was observed during GS-HNE stimulation and reached a maximum at 2 h ($P < 0.01$ vs. 0, 4 and 24 h by one-way ANOVA). The level of cysLTs returned to baseline by 4 h and thus the increase in cysLTs preceded the maximal infiltration of PMNs (see Figure 3). Importantly, GS-HNE alone showed no cross-reactivity in the ELISA for cysLTs (data not shown). Next, we performed mediator lipidomic profiling with exudates from GS-HNE-stimulated mice at 4 h post injection. As shown in Figure 6B, the pro-inflammatory lipid mediators LTB_4 and PGE_2 were identified by LC/MS/MS analysis based on their mass spectra and retention time directly compared with authentic standards. Additionally, thromboxane B_2, the stable hydrolysis product of pro-thrombotic thromboxane A_2, was identified in these exudates. Monohydroxy fatty acid products (5-, 15- and 12-HETE) were also identified as markers of lipoxygenase activity with endogenous arachidonate (Figure 6C). Of interest, 17-hydroxy-DHA (17-HDHA), which is a marker of the resolvin D-series pathway, was also present in exudates from GS-HNE-treated mice. A representative mass spectrum for 17-HDHA is shown in Figure 6D. Diagnostic ions as well as the chromatogram derived from multiple reaction monitoring (inset) are shown. Importantly, endogenous

D-series resolvins were not identified. Of note, LTB_4, thromboxane B_2 and 5-HETE were not detected in mice injected with saline alone and only low amounts of PGE_2 (0.14 ng per exudate), 15-HETE (0.095 ng per exudate), 12-HETE (0.29 ng per exudate) and 17-HDHA (0.29 ng per exudate) were generated.

RvD1 prevents GS-HNE-stimulated peritonitis

Acute inflammation is mounted by pro-inflammatory stimuli and subsequently spontaneously resolves, actions governed in part by lipid mediators such as the resolvins. During mediator lipidomic analyses of exudates obtained from GS-HNE-stimulated mice, we identified 17-HDHA, a marker of the resolvin pathway, but not RvD1. Accordingly, we hypothesized that anti-inflammatory and pro-resolving lipid mediator RvD1 might counteract the pro-inflammatory actions of GS-HNE *in vivo*. As shown in Figure 7A, i.v. administration of RvD1 (0.01–10.0 ng) immediately before i.p. administration of GS-HNE (10 µg) sharply reduced neutrophilic infiltration stimulated by GS-HNE. This reduction by RvD1 was robust (~70%) and significant at doses as low as 0.1 ng when compared with administration of GS-HNE plus vehicle. Peritoneal linings were taken for histological evaluation (haematoxylin and eosin stained) and confirmed the sharp decrease in leukocyte infiltration stimulated by RvD1 (Figure 7B, upper
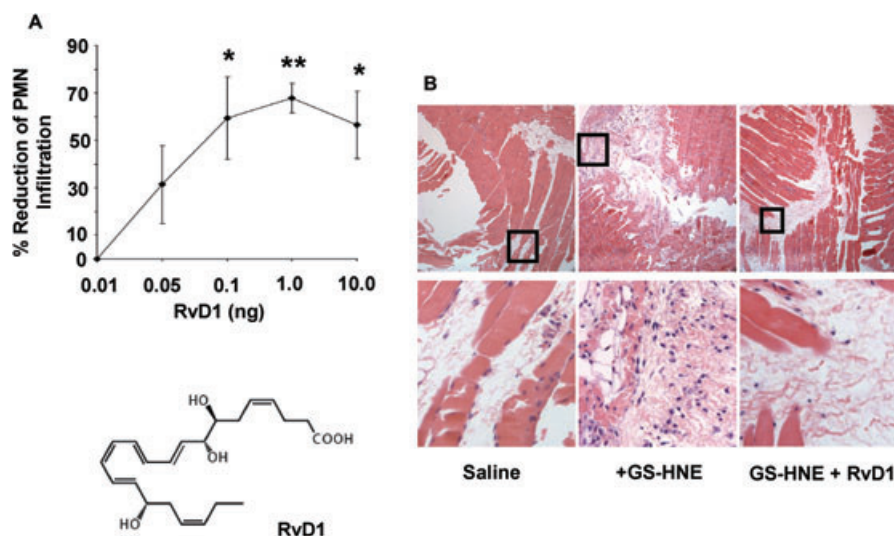
Figure 7 Resolvin D1 (RvD1) counters GS-HNE-stimulated peritonitis. Mice were injected i.v. with RvD1 (0.01–10.0 ng; A) immediately before administration of GS-HNE (10 µg intraperitoneally). After 4 h, the peritoneal cavity was lavaged and PMN numbers were determined (see *Methods*). Sections from the peritoneal lining (haematoxylin and eosin stained) obtained for histological analysis are shown in (B) (top; original magnification 10×) with increased magnification in the lower panels. Results are presented as mean ± SEM ($n = 3$–5), *$P < 0.05$, **$P < 0.01$. GS-HNE, glutathionyl-4-hydroxy-*trans*-2-nonenal; PMN, polymorphonuclear leukocyte.

panels at 10× magnification with increased magnification shown in the lower panels as indicated), consistent with the differential cell counts in exudates.

Discussion and conclusions

The present study describes the potential pro-inflammatory actions of the GSH conjugate of a lipid peroxidation product, HNE. This conjugate, GS-HNE, induced peritonitis in mice, resulting in the recruitment of leukocytes and the *in vivo* generation of pro-inflammatory lipid mediators, including PGs and LTs. The actions of GS-HNE were further illustrated with isolated human PMNs where GS-HNE stimulated both superoxide generation and surface expression of adhesion receptors. Notably, the inflammatory response induced by GS-HNE was mitigated by RvD1 *in vivo*. These results support the notion that GSH-dependent metabolism of reactive lipid peroxidation products, such as HNE, can result in local production of new pro-inflammatory mediators with novel bioactions.

The generation of HNE is associated with many chronic diseases characterized by high levels of inflammation, such as atherosclerosis, rheumatoid arthritis and allergic airway inflammation (Yla-Herttuala *et al.*, 1989; Selley *et al.*, 1992; Boldogh *et al.*, 2005). The blood plasma level of HNE reaches micromolar concentrations following ischaemia/reperfusion injury in humans and similar concentrations of HNE have been measured in many other human and animal studies (Strohmaier *et al.*, 1995; Siems and Grune, 2003). Although a number of studies have demonstrated a pro-inflammatory role for HNE, until now, the relative bioactivity of specific HNE metabolites was not established. Accordingly, in the present study, we provide direct evidence showing that glutathiolation of HNE confers remarkable pro-inflammatory properties on this α,β-unsaturated aldehyde.

Although HNE is metabolized via multiple pathways, glutathiolation is its primary metabolic fate, which represents 30–70% of HNE metabolism in a multitude of tissues and cell types, including vascular smooth muscle cells, erythrocytes and the heart (Srivastava *et al.*, 1998; 2000; 2001; Siems and Grune, 2003). The appearance of GS-HNE is used as a biomarker of oxidative stress and increased levels of GS-HNE are associated with chronic inflammatory diseases such as Alzheimer's disease (Volkel *et al.*, 2005; 2006). Results from several studies show that GSH-mediated metabolism of HNE protects against a multitude of toxic and potentially deleterious effects, such as preventing HNE-DNA adduct formation and HNE-induced neuronal toxicity (Xie *et al.*, 1998; Falletti *et al.*, 2007). However, in view of the high biological reactivity of GSH conjugates of other lipid-derived electrophiles (Samuelsson *et al.*, 1987), we sought to examine the role of glutathiolation in mediating the pro-inflammatory effects of HNE. Indeed, the results presented here demonstrate that GS-HNE is a more potent trigger of neutrophilic infiltration *in vivo* than non-conjugated HNE. It should be noted that although HNE has been shown to be a direct PMN chemoattractant *in vitro* (Curzio *et al.*, 1987; Schaur *et al.*, 1994), the lack of robust PMN infiltration following administration of HNE in the present studies may reflect its bioavailability given its high chemical reactivity (e.g. bound to serum proteins). Although HNE is rapidly metabolized to GS-HNE in a variety of cell types, including PMNs (Siems and Grune, 2003), the conversion of HNE to GS-HNE in this model is likely to be less efficient because of the route of administration and/or generation of secondary metabolites. In a key structure/function analysis, we also determined that reduction of the aldehyde moiety to the alcohol, GS-DHN, abolishes the bioactivity of GS-HNE. Reduction, mediated in extra-hepatic tissues primarily by aldose reductase, is a significant metabolic fate of HNE in many cell types (Srivastava *et al.*, 1998; 2000). Hence, overall, this relative bioactivity profile lends support to the

notion that further metabolism of the conjugate to GS-DHN is necessary to completely detoxify and inactivate HNE.

Among the products investigated herein (HNE and GS-DHN), GS-HNE was found to be the most potent pro-inflammatory stimulus *in vivo*. Hence, we further pursued this metabolite in order to define its bioactivity more rigorously. Intraperitoneal administration of GS-HNE caused an increase in PMN infiltration at a dose of just 1 µg per mouse (2.2 nmol or ~0.04 mg·kg^{-1}). In healthy rats, the concentration of the mercapturic acid conjugate of 1,4-dihydroxynonanol (DHN-MA, which is the major metabolite of GS-HNE in the urine) has been found to be approximately 0.15 nmol·day^{-1} (Rathahao *et al.*, 2005). Considering other metabolites of the conjugate, the total generation of GS-HNE in healthy rats would be between 0.5 and 0.8 nmol. In conditions of oxidative stress, the concentration of DHN-MA in the urine increases 10–15-fold (Kuiper *et al.*, 2008). Hence, the 2.2 nmol (1 µg) dose used in the study is likely to be within the concentration range of the conjugate generated *in vivo* during oxidative stress. For comparison, the pro-inflammatory effects of oxidized LDL *in vivo* appear at 100–200 times the dose of GS-HNE used here (Lehr *et al.*, 1991; Fuhrman *et al.*, 2008). The observation that the time course of PMN infiltration by GS-HNE is biphasic and that GS-HNE is rapidly cleared from the peritoneum suggests that perhaps other mediators generated by GS-HNE serve to amplify the inflammatory response *in vivo*. To identify potential amplifiers of the response to GS-HNE, we performed a lipidomic analysis of the exudates obtained from mice treated with GS-HNE. Stimulation with GS-HNE results in the generation of other known pro-inflammatory lipid mediators, such as LTB$_4$, thromboxane A$_2$ and PGE$_2$. Moreover, our *in vitro* results also demonstrate that GS-HNE has direct actions on PMNs. Using isolated human PMNs, GS-HNE led to an increase in superoxide generation at doses as low as 1 µmol·L^{-1} (0.0046 mg·mL^{-1}). Interestingly, oxidized LDL has also been shown to stimulate superoxide production by PMNs (Maeba *et al.*, 1995), but the doses required are over 100 times higher than that of GS-HNE used in the present study. It is of interest to point out that free HNE inhibits fMLP-induced respiratory burst (Dianzani *et al.*, 1996). Collectively, these observations suggest that glutathiolation could be viewed as a bioactivation step that transforms HNE into a more bioactive metabolite *in vivo*. To the best of our knowledge, this is the first demonstration that the GSH conjugate of HNE has inherent bioactivity greater than HNE itself.

To evaluate the potency of GS-HNE as an inducer of murine peritonitis, we compared GS-HNE at similar doses with well-known neutrophil chemoattractants and agonists, LTB$_4$ (Samuelsson *et al.*, 1987; Griswold *et al.*, 1991; Yedgar *et al.*, 2007) and fMLP (Molad *et al.*, 1994). Parallel analysis showed that PMN infiltration stimulated by GS-HNE was within the range of that stimulated by LTB$_4$ and fMLP. In contrast, GS-HNE alone did not significantly increase vascular permeability in a side-by-side comparison with LTD$_4$. Although this does not preclude the potential for direct actions on endothelial cells, it appears that within this concentration range, the primary actions of GS-HNE were on leukocytes. This is interesting in light of the fact that cysLTs increase vascular permeability, but are not direct neutrophil chemoattractants (Samuelsson *et al.*, 1987; Griswold *et al.*, 1991). Although action at the cysLT

receptors cannot be ruled out, it is likely that GS-HNE and cysLTs do not act via similar mechanisms *in vivo*, although they are both GSH-lipid conjugates. Of note, GS-HNE stimulates the production of cysLTs *in vivo* (Figure 6). As GS-HNE, like the cysLTs, is not likely to be cell-permeable, the present results suggest that GS-HNE actions *in vivo* are potentially receptor-mediated, but the receptors involved remain to be identified. The present results support the view that glutathiolation increases the bioactivity of HNE and raise the possibility that other reactive lipid metabolites could be activated by glutathiolation and sensed by components of the immune system. In this regard, it is significant to point out that in addition to LTC$_4$ and its metabolites (LTD$_4$ and LTE$_4$), other GSH-lipid conjugates, such as 5-oxo-glutathione (FOG$_7$), also demonstrate high biological activity (Bowers *et al.*, 2000; Yedgar *et al.*, 2007). Moreover, conjugation to GSH is a common metabolic fate of a variety of lipid-peroxidation products (e.g. isoprostanes), and thus the results presented here have broad implications and may be useful in identifying the biological activity of the GSH conjugates of other bioactive lipids and lipid-derived products (Milne *et al.*, 2004).

One of the key findings of this study is that the pro-inflammatory response initiated by GS-HNE *in vivo* was drastically reduced by the anti-inflammatory/pro-resolving lipid mediator, RvD1. The resolvins were initially identified in resolving exudates in murine models of acute inflammation and have been shown to exhibit potent biological actions in disease models, such as colitis, peritonitis and periodontitis (Serhan *et al.*, 2002; Serhan and Chiang, 2008). Recently, RvD1 was prepared by total organic synthesis, its stereochemistry was determined and it potently (low nanomolar range) reduced fMLP-stimulated transmigration of human PMNs *in vitro*, as well as zymosan A-stimulated murine peritonitis *in vivo* (Sun *et al.*, 2007). In the present report, we also identified 17-HDHA, a marker of the resolvin D-series pathway, in exudates of mice given GS-HNE. However, D-series resolvins were not identified in our mediator lipidomic analyses of exudate lavages and thus an uncoupling of the resolvin biosynthetic pathway could prolong the GS-HNE-stimulated inflammatory response. Thus, we hypothesized that resolvins could counteract the pro-inflammatory effects of GS-HNE *in vivo*. Accordingly, pre-treatment with RvD1 drastically reduced GS-HNE-stimulated peritoneal PMN infiltration at doses as low as just 50 pg per mouse. Collectively, these results, combined with earlier findings (Sun *et al.*, 2007; Serhan and Chiang, 2008), suggest that RvD1 has potent actions with regard to dampening inflammation that may be independent of the stimulus and demonstrate for the first time the novel role of RvD1 in counter-regulating oxidative stress-initiated inflammation. It should be noted that although relatively high concentrations of DHA are reported to protect against oxidative stress by serving a sacrificial role as a direct antioxidant (Yavin *et al.*, 2002), the present results indicate that enzymically derived potent mediators that are formed from DHA, such as RvD1, and are 100–1000× more potent and activate specific receptors in the low nanomolar range (Kasuga *et al.*, 2008), could mediate some of the protective actions of DHA via agonist signalling to counter the deleterious impact of oxidative stress.

In summary, the present results demonstrate a novel role for the GSH conjugate of HNE as a pro-inflammatory stimulus

and suggest that GS-HNE must be reduced further to abolish its bioactivity. Because oxidative stress is a generalized feature associated with many chronic inflammatory diseases, these results suggest that anti-inflammatory/pro-resolving lipid mediators, such as RvD1, can now provide novel therapeutic strategies for the management of oxidative stress-induced inflammation as well as associated pathological and toxicological states.

Acknowledgements

Conflict of interest disclosure

C.N.S. is the inventor on patents for resolvins assigned to Brigham and Women's Hospital and licensed for clinical development. These are the basis for consultantships for C.N.S.

References

Benedetti A, Comporti M, Esterbauer H (1980). Identification of 4-hydroxynonenal as a cytotoxic product originating from the peroxidation of liver microsomal lipids. *Biochim Biophys Acta* **620**: 281–296.

Boldogh I, Bacsi A, Choudhury BK, Dharajiya N, Alam R, Hazra TK *et al.* (2005). ROS generated by pollen NADPH oxidase provide a signal that augments antigen-induced allergic airway inflammation. *J Clin Invest* **115**: 2169–2179.

Bowers RC, Hevko J, Henson PM, Murphy RC (2000). A novel glutathione containing eicosanoid (FOG7) chemotactic for human granulocytes. *J Biol Chem* **275**: 29931–29934.

Cotran RS, Kumar V, Collins T (Eds) (1999). *Robbins Pathologic Basis of Disease*. Philidelphia: W.B. Saunders.

Curzio M, Esterbauer H, Poli G, Biasi F, Cecchini G, Di Mauro C *et al.* (1987). Possible role of aldehydic lipid peroxidation products as chemoattractants. *Int J Tissue React* **9**: 295–306.

Dianzani C, Parrini M, Ferrara C, Fantozzi R (1996). Effect of 4-hydroxynonenal on superoxide anion production from primed human neutrophils. *Cell Biochem Funct* **14**: 193–200.

Falletti O, Cadet J, Favier A, Douki T (2007). Trapping of 4-hydroxynonenal by glutathione efficiently prevents formation of DNA adducts in human cells. *Free Radic Biol Med* **42**: 1258–1269.

Fiore S, Serhan CN (1995). Lipoxin A4 receptor activation is distinct from that of the formyl peptide receptor in myeloid cells: inhibition of CD11/18 expression by lipoxin A4-lipoxin A4 receptor interaction. *Biochemistry* **34**: 16678–16686.

Fuhrman B, Partoush A, Volkova N, Aviram M (2008). Ox-LDL induces monocyte-to-macrophage differentiation in vivo: Possible role for the macrophage colony stimulating factor receptor (M-CSF-R). *Atherosclerosis* **196**: 598–607.

Griswold DE, Webb EF, Hillegass LM (1991). Induction of plasma exudation and inflammatory cell infiltration by leukotriene C4 and leukotriene B4 in mouse peritonitis. *Inflammation* **15**: 251–258.

Hasturk H, Kantarci A, Ohira T, Arita M, Ebrahimi N, Chiang N *et al.* (2006). RvE1 protects from local inflammation and osteoclast-mediated bone destruction in periodontitis. *Faseb J* **20**: 401–403.

Hong S, Porter TF, Lu Y, Oh SF, Pillai PS, Serhan CN (2008). Resolvin E1 metabolome in local inactivation during inflammation-resolution. *J Immunol* **180**: 3512–3519.

Kasuga K, Yang R, Porter TF, Agrawal N, Petasis NA, Irimia D *et al.* (2008). Rapid appearance of resolvin precursors in inflammatory exudates: Novel mechanisms in resolution. *J Immunol* **181**: 8677–8687.

Kuiper HC, Miranda CL, Sowell JD, Stevens JF (2008). Mercapturic acid conjugates of 4-hydroxy-2-nonenal and 4-oxo-2-nonenal metabolites are in vivo markers of oxidative stress. *J Biol Chem* **283**: 17131–17138.

Lehr HA, Hubner C, Finckh B, Angermuller S, Nolte D, Beisiegel U *et al.* (1991). Role of leukotrienes in leukocyte adhesion following systemic administration of oxidatively modified human low density lipoprotein in hamsters. *J Clin Invest* **88**: 9–14.

Libby P (2007). Inflammatory mechanisms: the molecular basis of inflammation and disease. *Nutr Rev* **65**: S140–S146.

Maeba R, Maruyama A, Tarutani O, Ueta N, Shimasaki H (1995). Oxidized low-density lipoprotein induces the production of superoxide by neutrophils. *FEBS Lett* **377**: 309–312.

Milne GL, Zanoni G, Porta A, Sasi S, Vidari G, Musiek ES *et al.* (2004). The cyclopentenone product of lipid peroxidation, 15-A2t-isoprostane, is efficiently metabolized by HepG2 cells via conjugation with glutathione. *Chem Res Toxicol* **17**: 17–25.

Molad Y, Haines KA, Anderson DC, Buyon JP, Cronstein BN (1994). Immunocomplexes stimulate different signalling events to chemoattractants in the neutrophil and regulate L-selectin and beta 2-integrin expression differently. *Biochem J* **299** (Pt 3): 881–887.

Ramana KV, Bhatnagar A, Srivastava S, Yadav UC, Awasthi S, Awasthi YC *et al.* (2006). Mitogenic responses of vascular smooth muscle cells to lipid peroxidation-derived aldehyde 4-hydroxy-trans-2-nonenal (HNE): role of aldose reductase-catalyzed reduction of the HNE-glutathione conjugates in regulating cell growth. *J Biol Chem* **281**: 17652–17660.

Rathahao E, Peiro G, Martins N, Alary J, Gueraud F, Debrauwer L (2005). Liquid chromatography-multistage tandem mass spectrometry for the quantification of dihydroxynonene mercapturic acid (DHN-MA), a urinary end-metabolite of 4-hydroxynonenal. *Anal Bioanal Chem* **381**: 1532–1539.

Samuelsson B, Dahlen SE, Lindgren JA, Rouzer CA, Serhan CN (1987). Leukotrienes and lipoxins: structures, biosynthesis, and biological effects. *Science* **237**: 1171–1176.

Schaur RJ, Dussing G, Kink E, Schauenstein E, Posch W, Kukovetz E *et al.* (1994). The lipid peroxidation product 4-hydroxynonenal is formed by–and is able to attract–rat neutrophils in vivo. *Free Radic Res* **20**: 365–373.

Selley ML, Bourne DJ, Bartlett MR, Tymms KE, Brook AS, Duffield AM *et al.* (1992). Occurrence of (E)-4-hydroxy-2-nonenal in plasma and synovial fluid of patients with rheumatoid arthritis and osteoarthritis. *Ann Rheum Dis* **51**: 481–484.

Serhan CN, Chiang N (2008). Endogenous pro-resolving and anti-inflammatory lipid mediators: a new pharmacologic genus. *Br J Pharmacol* **153** (Suppl. 1): S200–S215.

Serhan CN, Hong S, Gronert K, Colgan SP, Devchand PR, Mirick G *et al.* (2002). Resolvins: a family of bioactive products of omega-3 fatty acid transformation circuits initiated by aspirin treatment that counter proinflammation signals. *J Exp Med* **196**: 1025–1037.

Serhan CN, Brain SD, Buckley CD, Gilroy DW, Haslett C, O'neill LA *et al.* (2007a). Resolution of inflammation: state of the art, definitions and terms. *Faseb J* **21**: 325–332.

Serhan CN, Lu Y, Hong S, Yang R (2007b). Mediator lipidomics: search

algorithms for eicosanoids, resolvins, and protectins. *Methods Enzymol* **432**: 275–317.

Siems W, Grune T (2003). Intracellular metabolism of 4-hydroxynonenal. *Mol Aspects Med* **24**: 167–175.

Siems WG, Zollner H, Grune T, Esterbauer H (1997). Metabolic fate of 4-hydroxynonenal in hepatocytes: 1,4-dihydroxynonene is not the main product. *J Lipid Res* **38**: 612–622.

Srivastava S, Chandra A, Wang LF, Seifert WE Jr, Dague BB, Ansari NH *et al.* (1998). Metabolism of the lipid peroxidation product, 4-hydroxy-trans-2-nonenal, in isolated perfused rat heart. *J Biol Chem* **273**: 10893–10900.

Srivastava S, Conklin DJ, Liu SQ, Prakash N, Boor PJ, Srivastava SK *et al.* (2001). Identification of biochemical pathways for the metabolism of oxidized low-density lipoprotein derived aldehyde-4-hydroxy trans-2-nonenal in vascular smooth muscle cells. *Atherosclerosis* **158**: 339–350.

Srivastava S, Dixit BL, Cai J, Sharma S, Hurst HE, Bhatnagar A *et al.* (2000). Metabolism of lipid peroxidation product, 4-hydroxynonenal (HNE) in rat erythrocytes: role of aldose reductase. *Free Radic Biol Med* **29**: 642–651.

Strohmaier H, Hinghofer-Szalkay H, Schaur RJ (1995). Detection of 4-hydroxynonenal (HNE) as a physiological component in human plasma. *J Lipid Mediat Cell Signal* **11**: 51–61.

Subbanagounder G, Watson AD, Berliner JA (2000). Bioactive products of phospholipid oxidation: isolation, identification, measurement and activities. *Free Radic Biol Med* **28**: 1751–1761.

Sun YP, Oh SF, Uddin J, Yang R, Gotlinger K, Campbell E *et al.* (2007).

Resolvin D1 and its aspirin-triggered 17R epimer. Stereochemical assignments, anti-inflammatory properties, and enzymatic inactivation. *J Biol Chem* **282**: 9323–9334.

Volkel W, Alvarez-Sanchez R, Weick I, Mally A, Dekant W, Pahler A (2005). Glutathione conjugates of 4-hydroxy-2(E)-nonenal as biomarkers of hepatic oxidative stress-induced lipid peroxidation in rats. *Free Radic Biol Med* **38**: 1526–1536.

Volkel W, Sicilia T, Pahler A, Gsell W, Tatschner T, Jellinger K *et al.* (2006). Increased brain levels of 4-hydroxy-2-nonenal glutathione conjugates in severe Alzheimer's disease. *Neurochem Int* **48**: 679–686.

Winyard PG, Willoughby DA (Eds) (2003). *Inflammation Protocols*. Totowa, NJ: Humana Press.

Xie C, Lovell MA, Markesbery WR (1998). Glutathione transferase protects neuronal cultures against four hydroxynonenal toxicity. *Free Radic Biol Med* **25**: 979–988.

Yavin E, Brand A, Green P (2002). Docosahexaenoic acid abundance in the brain: a biodevice to combat oxidative stress. *Nutr Neurosci* **5**: 149–157.

Yedgar S, Krimsky M, Cohen Y, Flower RJ (2007). Treatment of inflammatory diseases by selective eicosanoid inhibition: a double-edged sword? *Trends Pharmacol Sci* **28**: 459–464.

Yla-Herttuala S, Palinski W, Rosenfeld ME, Parthasarathy S, Carew TE, Butler S *et al.* (1989). Evidence for the presence of oxidatively modified low density lipoprotein in atherosclerotic lesions of rabbit and man. *J Clin Invest* **84**: 1086–1095.